Photoionization of palladium including relaxation effects

M. Kutzner and S. E. Vance
Physics Department, Andrews University, Berrien Springs, Michigan 49104
(Received 5 July 1994)

Total and partial photoionization cross sections, branching ratios, and angular-distribution asymmetry parameters for the 4*d*, 4*p*, 4*s*, and 3*d* subshells of palladium have been calculated using the relativistic random-phase approximation and the relativistic random-phase approximation modified to include relaxation effects. Comparisons are made between results that include relaxation effects and those that do not. Minor relaxation effects are noted for the 4*d* and 3*d* photoionization parameters. However, substantial relaxation effects are noted for both the 4*p* and 4*s* subshells. Large relaxation effects are observed in the 4*p* partial cross section and branching ratio. Also observed is the appearance of a Cooper minimum in the 4*s* photoionization cross section and a corresponding change in the 4*s* angular-distribution asymmetry parameter.

PACS number(s): 32.80.Fb, 32.80.Hd

I. INTRODUCTION

The study of photoionization of inner shells of many elements has led to an increased understanding of a number of many-body phenomena including relaxation and polarization effects, the Auger effect, photoionization-with-excitation, and multiple photoionization. The importance of relaxation has long been established in the photoionization of 3*d* and 4*d* subshells of elements xenon ($Z=54$) through the lanthanides. Previous studies employing the relativistic random-phase approximation modified to include relaxation effects (RRPAR) of the alkaline-earth-metal atoms group-IIA atoms [1], group-IIB atoms [2], and Yb ($Z=70$) [3], have investigated the effects of relaxation in many closed-shell systems. Photoionization cross sections from *nd* subshells (especially the 4*d* subshells) were shown to be significantly influenced by the relaxation effects, and the 4*f* cross section of mercury was brought into good agreement with experiment when relaxation effects were included [2].

Paladium ($Z=46$) is the only atom with a valence 4*d* subshell. Previous photoionization studies of palladium have been carried out by Amusia and Cherepkov using the random-phase approximation with exchange (RPAE) [4] and by Radojević and Johnson [5], followed by Shanthi and Deshmukh [6], using the relativistic random-phase approximation (RRPA). Little experimental data on photoionization of palladium has been reported. Several members of the Rydberg series and members of the autoionizing [$4d^9(^2D_{3/2,5/2})np$ and nf] levels have been studied by Karamatskos *et al.* [7] and Baig [8]. Spectroscopic data for some excited bound states was obtained by Moore [9].

In this paper, we report on the effects of core relaxation on the photoionization of 4*d*, 4*p*, 4*s*, and 3*d* electrons of palladium. In Sec. II, we briefly review the methods of the RRPAR. The results for the 4*d*, 4*p*, 4*s*, and 3*d* subshells are reported in Sec. III. Section IV is a brief discussion of some of the implications of the work.

II. METHODS

Detailed discussions of both the RRPA [10] and the RRPAR [11] methods can be found elsewhere. Here, we point out that in the RRPA, the partial photoionization cross section for a given subshell is given by

$$\sigma_{n\kappa}=\frac{4\pi^2\alpha\omega}{3}(|D_{nj\to j-1}|^2+|D_{nj\to j}|^2+|D_{nj\to j+1}|^2)\ , \quad (1)$$

where n is the principal quantum number and $\kappa=\mp(j+1/2)$ for $j=l\pm\frac{1}{2}$, where j and l are the single-electron total and orbital angular-momentum quantum numbers, respectively. The dipole matrix element $D_{nj\to j'}$ is the reduced RRPA dipole matrix element for the photoionization channel $nj\to j'$.

The angular-distribution asymmetry parameter $\beta_{n\kappa}$ for the subshell $n\kappa$ is defined in terms of the differential photoionization cross section as

$$\frac{d\sigma_{n\kappa}}{d\Omega}=\frac{\sigma_{n\kappa}(\omega)}{4\pi}[1-\tfrac{1}{2}\beta_{n\kappa}(\omega)P_2(\cos(\theta))]\ , \quad (2)$$

where ω is the photon energy and θ is the angle measured between the directions of the incident photon and the photoelectron. When a subshell is split by spin-orbit splitting into two different levels κ and κ', it is conventional to use the weighted average given by

$$\beta_{n\kappa}=\frac{\sigma_{n\kappa}\beta_{n\kappa}+\sigma_{n\kappa'}\beta_{n\kappa'}}{\sigma_{n\kappa}+\sigma_{n\kappa'}}\ . \quad (3)$$

The RRPAR method approximates the effects of core relaxation by calculating the continuum photoelectron orbitals in the potential of the relaxed ion. The ionic core with the hole in the level with $j=l+\frac{1}{2}$ has a lower ionization threshold energy and also represents the most populated of the two levels. Thus, we generally consider the hole to be in the subshell with largest j for the purpose of obtaining the V^{N-1} potential. Overlap integrals of the form $\prod_i\langle\phi_i'|\phi_i\rangle^{q_i}$ between orbitals of the unre-

laxed ground state ϕ_i and the corresponding orbitals of the final relaxed state ϕ_i' are included in the RRPAR dipole matrix element for each subshell i of the ion with occupation number q_i. Inclusion of these overlap integrals is important for calculations of partial photoionization cross sections since they approximately remove oscillator strength due to double-excitation processes from the single-excitation channel oscillator strength [12]. It should be noted that overlap integrals between orbitals of the ground state and the continuum orbitals of the final state have not been included. Thus, oscillator strength due to Auger processes has not been removed from the mainline partial cross sections.

Photoionization thresholds in the strict RRPA model are the Dirac-Hartree-Fock (DHF) eigenvalues [10]. However, experimental thresholds are frequently utilized. Here, we have used DHF threshold energies for RRPA calculations. In the RRPAR, we have used experimental ionization energies [9] for the calculations involving relaxation of the $4d$ hole. For calculations of other channels including relaxation, the difference in the total relativistic self-consistent energies of the neutral atom and the ion (so-called $\Delta E_{\rm SCF}$ energies) were used. The DHF and $\Delta E_{\rm SCF}$ energies used in these calculations were obtained using the Oxford multiconfiguration Dirac-Fock computer code of Grant *et al.* [13]. Table I contains DHF, $\Delta E_{\rm SCF}$, and experimental threshold energies obtained using photoelectron spectroscopy for all the channels incorporated in the present study.

The RRPA theory predicts results that are gauge independent provided that one has included all possible dipole-excited channels [10]. In practice, where one limits the number of channels (the truncated RRPA), there will be differences between the "length-" and "velocity-" gauge results. Also, the inclusion of relaxation effects in the RRPAR potential leads to differences in calculations performed in the two gauges. In this paper, the geometric means of length and velocity cross sections are generally shown for the RRPA where they are nearly indistinguishable. For RRPAR results, we show both length and velocity separately.

TABLE I. Photoionization thresholds in a.u. for subshells of atomic palladium included in the present calculations. The third column lists the absolute values of single-particle eigenvalues from DHF calculations. The fourth column lists the differences of self-consistent DHF calculations for the ground states and ionic states. The experimental values are from Ref. [9].

Shell	J	Thresholds DHF	$\Delta E_{\rm SCF}$	Expt.
$4d$	5/2	0.3198	0.2305	0.3063
$4d$	3/2	0.3405	0.2464	0.3225
$4p$	3/2	2.347	2.185	
$4p$	1/2	2.520	2.348	
$4s$	1/2	3.842	3.646	
$3d$	5/2	13.11	12.49	
$3d$	3/2	13.32	12.70	
$3p$	3/2	20.43	19.85	
$3p$	1/2	21.49	20.90	
$3s$	1/2	25.54	24.96	

The jj-coupled channels included in the RRPA and RRPAR calculations were as follows:

$$4d_{5/2} \rightarrow \epsilon f_{7/2}, \epsilon f_{5/2}, \epsilon p_{3/2} ,$$

$$4d_{3/2} \rightarrow \epsilon f_{5/2}, \epsilon p_{3/2}, \epsilon p_{1/2} ,$$

$$4p_{3/2} \rightarrow \epsilon d_{5/2}, \epsilon d_{3/2}, \epsilon s_{1/2} ,$$

$$4p_{1/2} \rightarrow \epsilon d_{3/2}, \epsilon s_{1/2} ,$$

$$4s_{1/2} \rightarrow \epsilon p_{3/2}, \epsilon p_{1/2} ,$$

for channels originating from the $n=4$ shell. For the $3d$ channels, we used

$$3d_{5/2} \rightarrow \epsilon f_{7/2}, \epsilon f_{5/2}, \epsilon p_{3/2} ,$$

$$3d_{3/2} \rightarrow \epsilon f_{5/2}, \epsilon p_{3/2}, \epsilon p_{1/2} ,$$

$$3p_{3/2} \rightarrow \epsilon d_{5/2}, \epsilon d_{3/2}, \epsilon s_{1/2} ,$$

$$3p_{1/2} \rightarrow \epsilon d_{3/2}, \epsilon s_{1/2} ,$$

$$3s_{1/2} \rightarrow \epsilon p_{3/2}, \epsilon p_{1/2} .$$

III. RESULTS

Numerous theoretical studies involving cadmium ($Z=48$) [2], negative iodine ($Z=53$) [14], xenon ($Z=54$) [15], cesium ($Z=55$) [16], barium ($Z=56$) [11], and lanthanum [17] have shown that relaxation and polarization are important many-body effects in photoionization from the $4d$ subshell in those systems. Since palladium is the only element with an outer $4d$ subshell, it is of interest to see what correlation effects are important there. The partial $4d$ photoionization cross sections above threshold are shown in Fig. 1(a) for the RPAE [4], RRPA, and RRPAR approximations. The RRPA result shown here is the geometric mean of length and velocity and is consistent with that reported previously by Shanthi and Deshmukh [6]. The RRPAR calculation is not gauge independent, thus, both length and velocity results are shown individually. The RRPA and RRPAR cross sections are not reported below the $4p$ thresholds where autoionization resonances complicate the computational procedure.

It is apparent from Fig. 1(a) that the effects of relaxation are not large for the valence shell photoionization of palladium. The peak of the cross section has been somewhat reduced and some of the oscillator strength has been displaced to energies above the $4p$ threshold, but the differences are not large. Evidently strong rearrangement effects depend on the presence of an outer subshell of spectator electrons whose orbitals will be significantly altered by the absence of an innershell electron. Neither the angular-distribution asymmetry parameter nor the branching ratio shown in Figs. 1(b) and 1(c) are strongly affected by the inclusion of relaxation either. In Fig. 1(d), we show the partitioning of the total cross section into partial $4d_{5/2}$, $4d_{3/2}$, and $4p$ cross sections. The inclusion

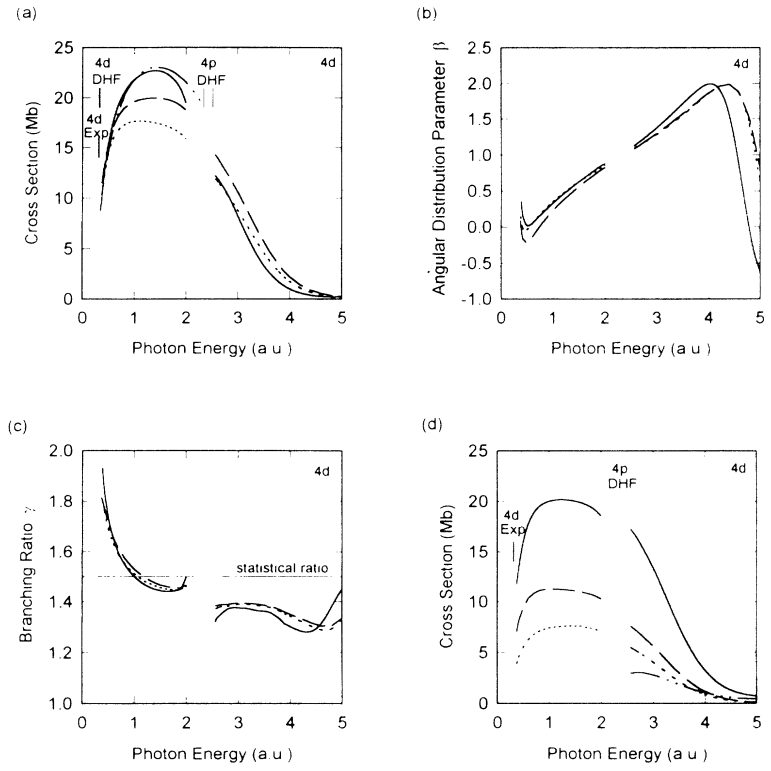

FIG. 1. Photoionization parameters for the $4d$ subshell of palladium. (a) Partial photoionization cross sections with the geometric mean of RRPA represented by the solid line and the RRPAR length and velocity calculations represented by the dashed and dotted lines, respectively. RPAE cross sections [4] are represented by the chain line. (b) Calculations of the angular-distribution asymmetry parameter β_{4d} are shown for the RRPA length (solid line), RRPAR length (dashed line), and RRPAR velocity (dotted line). (c) Calculations of the branching ratio γ are shown for the geometric mean of RRPA (solid line), RRPAR length (dashed line), and RRPAR velocity (dotted line). The statistical ratio is also plotted (horizontal solid line). (d) Partitioning of total cross section in RRPAR. Total cross section (solid line), the partial $4d_{5/2}$ cross section (dashed line), the partial $4d_{3/2}$ cross section (dotted line), and the sum of $4p$ and $4s$ partial cross sections (chain line). Geometric means of length and velocity results have been taken. DHF thresholds used in the RRPA and experimental (Exp) thresholds [9] used in the RRPAR are shown with their subshells.

of overlap integrals in the RRPAR calculations have reduced the partial $4d$ cross section by approximately 7%. It can also be noted that comparison with the RPAE [4], which is similar to the RRPA but nonrelativistic, shows that relativistic effects included in the RRPA reduce the cross section beyond the peak.

The penultimate $4p$ subshell photoionization cross section is shown in Fig. 2(a) and shows a very strong dependence on core relaxation. The unrelaxed RRPA result has the characteristic shape to be found for photoionization from inner p levels of many atoms. The RRPAR result, however, is considerably lower near threshold. The

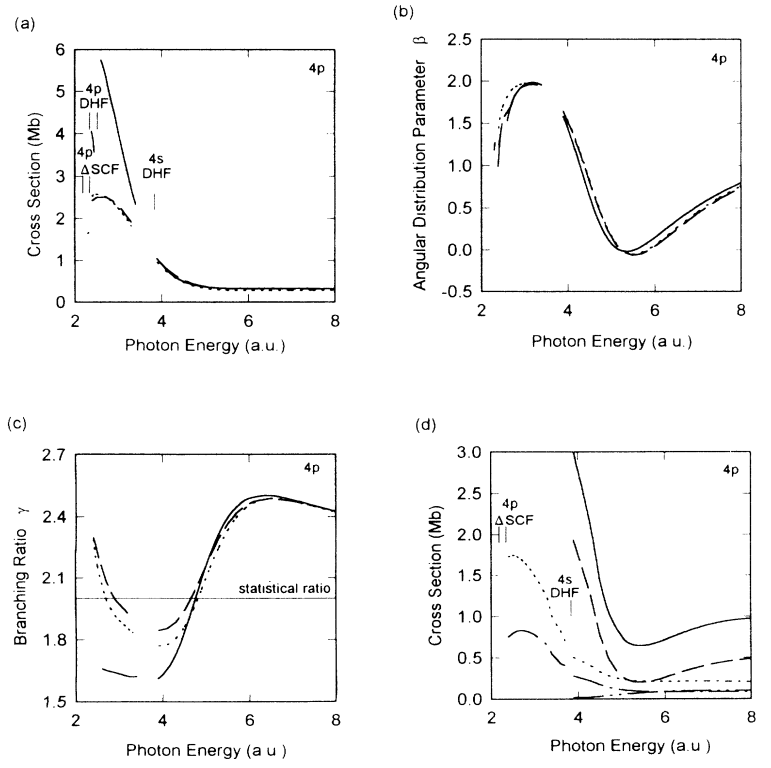

FIG. 2. Photoionization parameters for the $4p$ subshell of palladium. (a) Partial photoionization cross sections with the geometric mean of RRPA represented by the solid line and the RRPAR length and velocity calculations represented by the dashed and dotted lines, respectively. (b) Calculations of the angular-distribution asymmetry parameter β_{4p} are shown for the RRPA length (solid line), RRPAR length (dashed line), and RRPAR velocity (dotted line). (c) Calculations of the branching ratio γ are shown for the geometric mean of RRPA (solid line), RRPAR length (dashed line), and RRPAR velocity (dotted line). The statistical ratio is also plotted (horizontal solid line). (d) Partitioning of total cross section in RRPAR. Total cross section (solid line), the partial $4d$ cross section (dashed line), the partial $4p_{3/2}$ cross section (dotted line), the partial $4p_{1/2}$ (dot-dashed line), and the $4s$ partial cross sections (double-dot-dashed line). Geometric means of length and velocity results have been taken. DHF thresholds used in the RRPA and difference between DHF energy of neutral atom and ion (ΔSCF) thresholds used in the RRPAR are shown with their subshells.

result including relaxation shows a peak in the cross section just above threshold, which is only 44% of the RRPA cross section at 2.6 a.u. Part of this reduction in oscillator strength (approximately 9%) is due to the inclusion of overlap integrals between relaxed orbitals of the final state and unrelaxed orbitals of the initial state. The remainder of the reduction in cross section is due to changes in the photoelectron potential due to relaxation effects. Here cross sections are also shown for a region between the $4p_{3/2}$ and $4p_{1/2}$ thresholds.

The angular-distribution asymmetry parameter for the $4p$ subshell, β_{4p}, is shown in Fig. 2(b). There are few differences to be noted between the RRPA and RRPAR calculations. Other workers [6] have previously reported results of an RRPA calculation that are in disagreement with the present results. Whereas the present calculation varies between the values of zero and the upper theoretical limit of 2.0, the previously reported work [6] varies from approximately 1.4 to 2.4.

Considerable differences may be noted between the RRPAR and the RRPA calculations for the $\gamma=\sigma(4p_{3/2})/\sigma(4p_{1/2})$ branching ratio shown in Fig. 2(c). The initial deviations of γ from the statistical ratio are caused by the spin-orbit splitting of the $4p_{3/2}$ and $4p_{1/2}$ thresholds. Since the RRPA partial cross sections are initially decreasing toward a Cooper minimum, γ begins well below the statistical ratio of two. The RRPAR partial cross sections initially increase to a maximum above the thresholds leading to a value for γ greater than two. The RRPAR branching ratio then decreases to a value below two until the Cooper minimum is reached. In Fig. 2(d), we show the total cross section and the various single-excitation partial cross sections in the region above the $4p$ thresholds in the RRPAR.

The $4s$ partial photoionization cross section shown in Fig. 3(a) reveals interesting differences between the calculation including relaxation (RRPAR) and that which does not (RRPA). Immediately above threshold, the RRPAR cross section initially exhibits a minimum. This minimum is not predicted by the RRPA calculations, however, the RRPA results suggest that a Cooper minimum may reside in the discrete region below threshold [6]. Inclusion of overlap integrals in the RRPAR calculation reduces the $4s$ partial cross section by approximately 10.6%. Both the RRPA and RRPAR calculations of the angular-distribution asymmetry parameter, β_{4s}, [Fig. 3(b)] show large departures from the nonrelativistic value of 2.0 just above threshold. The magnitude of the departure is considerably less for the RRPAR than for the RRPA calculations.

Partial photoionization cross sections from the $3d$ subshell in both the RRPA and RRPAR are shown in Fig. 4(a). Note that the channels coupled in this calculation are different for the $3d$ subshell than for the outer subshells (see Sec. II). Although the RRPAR calculation yields a slightly broader peak than the RRPA result, most of the reduction is due to the inclusion of overlap integrals. The overlap integrals amount to approximately a 17% reduction in the $3d$ partial cross section. The angular-distribution asymmetry parameters, β_{3d}, for the $3d$ subshell are shown in Fig. 4(b). The effect of including relaxation is to lower and broaden the peak in the β parameter.

The branching ratios, $\gamma=\sigma(3d_{5/2})/\sigma(3d_{3/2})$, are shown in Fig. 4(c). Spin-orbit splitting of the $3d$ thresholds leads to deviations of the branching ratio from the statistical ratio of 3:2. Since the RRPAR partial cross sections have a reduced slope just above threshold relative to the RRPA, the RRPAR branching ratio does not reach as large a value as the RRPA.

The total photoionization cross section is shown in Fig. 4(d) along with the $3d_{5/2}$, $3d_{3/2}$, and sum of all other single-excitation $n=3$ and $n=4$ partial cross sections as calculated in the RRPAR. The contributions due to $3d$, $3p$, and $3s$ subshells are from an RRPAR calculation, which coupled all of the $n=3$ subshells. The contributions from $n=4$ channels were obtained from an RRPAR calculation coupling photoionization channels from $n=4$ shell and the $3d$ subshell. This assumes that couplings between $3s$ and $3p$ channels with $n=4$ shell

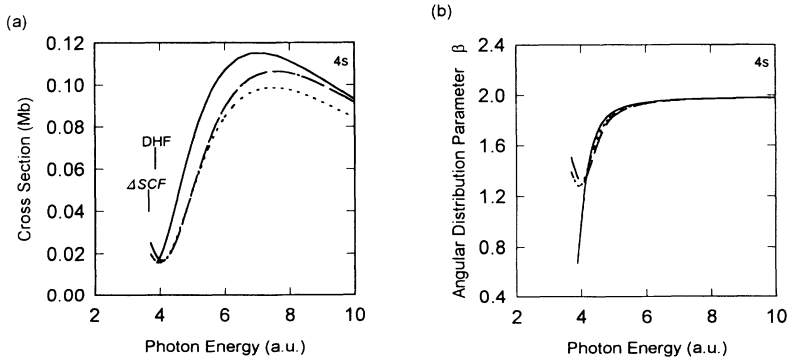

FIG. 3. Photoionization parameters for $4s$ subshell of palladium. (a) Partial photoionization cross sections with the geometric mean of RRPA represented by the solid line and the RRPAR length and velocity calculations represented by the dashed and dotted lines, respectively. DHF thresholds used in the RRPA and difference between DHF energy of neutral atom and ion (Δ SCF) thresholds used in the RRPAR are indicated. (b) Calculations of the angular-distribution asymmetry parameter β_{4s} are shown for the RRPA length (solid line), RRPAR length (dashed line), and RRPAR velocity (dotted line).

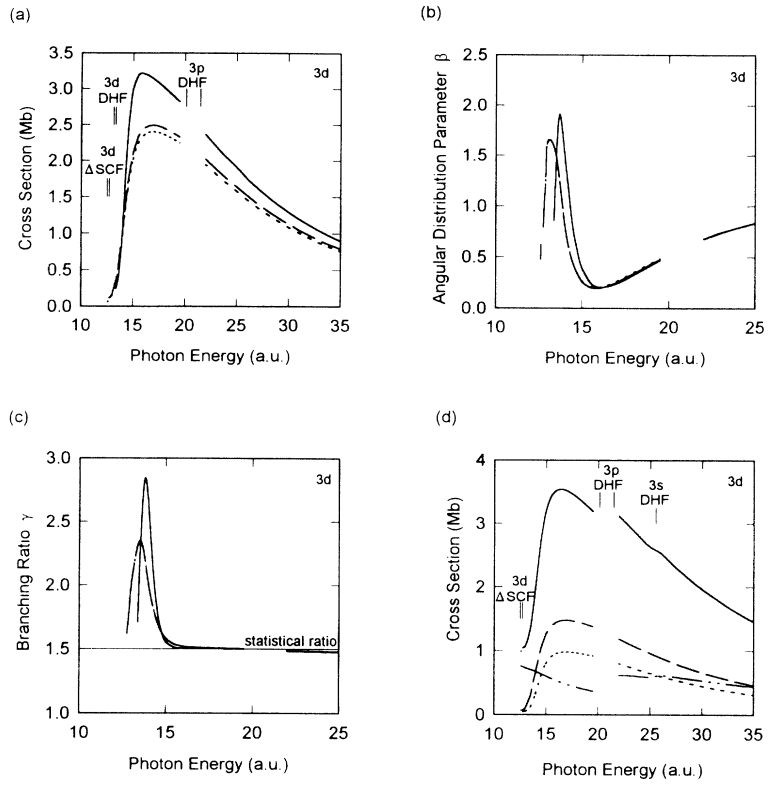

FIG. 4. Photoionization parameters for the $3d$ subshell of palladium. (a) Partial photoionization cross sections with the geometric mean of RRPA represented by the solid line and the RRPAR length and velocity calculations represented by the dashed and dotted lines, respectively. (b) Calculations of the angular-distribution asymmetry parameter β_{3d} are shown for the RRPA length (solid line), RRPAR length (dashed line), and RRPAR velocity (dotted line). (c) Calculations of the branching ratio γ are shown for the geometric mean of RRPA (solid line), RRPAR length (dashed line), and RRPAR velocity (dotted line). The statistical ratio is also plotted (horizontal solid line). (d) Partitioning of total cross section in RRPAR. Total cross section (solid line), the partial $3d_{5/2}$ cross section (dashed line), the partial $3d_{3/2}$ cross section (dotted line), and the sum of the single-excitation channels from $4d$, $4p$, $4s$, $3p$, and $3s$ subshells (double-dot-dashed line). Geometric means of length and velocity results have been taken. DHF thresholds and difference between DHF energy of neutral atom and ion (Δ SCF) thresholds used in the RRPAR are shown with their subshells.

channels are small and was done to reduce the already heavy demands on compute resources necessary to carry out the calculations.

IV. CONCLUSION

The calculations presented in this paper have evaluated the effects of core relaxation on the photoionization parameters for various subshells of the palladium atom. Whereas studies of other atomic systems have shown that relaxation effects are often substantial for inner subshells with large angular momentum, this study finds minor rearrangement effects for the $4d$ and $3d$ channels and large effects for the $4p$ and $4s$ inner subshell channels. This should not be surprising. The $4d$ subshell, being the valence subshell, will not undergo a great deal of rearrangement when one of its own members is removed, since there was only partial screening in the neutral atom. The $4p$ and $4s$ electrons, being interior, cause a more radical rearrangement of the somewhat loosely bound and populous $4d$ valence subshell, which leads to a modification of the photoelectron potential. The photoionization cross section for the $3d$ subshell peaks at energies well above threshold, so that the photoelectrons are not in the vicinity of the atom long enough to be strongly affected by many-body effects in the potential. Experimental verification of these results is greatly needed.

The results presented in this paper have not included the effects of core polarization. The importance of such effects on photoionization has been demonstrated in xenon [18] and barium [18,19]. It would be interesting to investigate how polarization alters the palladium cross sections.

ACKNOWLEDGMENTS

We wish to thank Walter Johnson for the use of the RRPA computer code and Vojislav Radojević for the use of the RRPAR code. This work was supported by NSF Grant No. PHY-9014012.

[1] M. Kutzner, D. Winn, and S. Mattingly, Phys. Rev. A **48**, 404 (1993).
[2] M. Kutzner, C. Tidwell, S. E. Vance, and V. Radojević, Phys. Rev. A **49**, 300 (1994).
[3] M. Kutzner and V. Radojević, Phys. Rev. A **49**, 2574 (1994).
[4] M. Ya. Amusia and N. A. Cherepkov, Case Stud. At. Phys. **5**, 47 (1975).
[5] V. Radojević and W. R. Johnson, J. Phys. B **16**, 177 (1983).
[6] N. Shanthi and P. C. Deshmukh, J. Phys. B **23**, 61 (1990).
[7] N. Karamatskos, M. Muller, M. Schmidt, and P. Zimmermann, Phys. Lett. A **102**, 409 (1984).
[8] M. A. Baig, J. Phys. B **21**, L365 (1988).
[9] C. E. Moore, *Atomic Energy Levels,* Natl. Bur. Stand. (U.S.) Circ. No. NSRDS-NBS 35, (U.S. GPO, Washington,

D.C., 1971), Vol. 3.
[10] W. R. Johnson and C. D. Lin, Phys. Rev. A **20**, 964 (1979); W. R. Johnson, C. D. Lin, K. T. Cheng, and C. M. Lee, Phys. Scr. **21**, 403 (1980).
[11] V. Radojević, M. Kutzner, and H. P. Kelly, Phys. Rev. A **40**, 727 (1989).
[12] T. Åberg, in *Photoionization and Other Probes of Many-Electron Interactions,* edited by F. Wuilleumier (Plenum, New York, 1976), pp. 49–59.
[13] I. P. Grant, B. J. McKenzie, P. H. Norrington, D. F. Mayers, and N. C. Pyper, Comput. Phys. Commun. **21**, 207 (1980).
[14] V. Radojević and H. P. Kelly, Phys. Rev. A **46**, 662 (1992).
[15] M. Kutzner, V. Radojević, and H. P. Kelly, Phys. Rev. A **40**, 5052 (1989).
[16] M. Ya. Amusia, N. A. Cherepkov, Dj. Živanović, and V. Radojević, Phys. Rev. A **13**, 1466 (1976).
[17] M. Ya. Amusia and S. I. Sheftel, Phys. Lett. A **55**, 469 (1976).
[18] M. Ya. Amusia, L. V. Chernysheva, G. F. Gribakin, and K. L. Tsemekhman, J. Phys. B At. Mol. Opt. Phys. **23**, 393 (1990).
[19] M. Kutzner, Z. Altun, and H. P. Kelly, Phys. Rev. A **41**, 3612 (1990).